

# Microstructure and Morphology of Amine-Cured Epoxy Coatings Before and After Outdoor Exposures—An AFM Study

Xiaohong Gu,\*\* Tinh Nguyen, Mounira Oudina, David Martin, Bouchra Kidah, Joan Jasmin, Aziz Rezig, Lipiin Sung, Eric Byrd, and Jonathan W. Martin—National Institute of Standards and Technology (NIST)\*  
Derek L. Ho—NIST Center for Neutron Research†  
Y.C. Jean—University of Missouri—Kansas City\*\*

*Atomic force microscopy (AFM) has been used to study the morphology and microstructure of an amine-cured epoxy before and after outdoor exposure. Measurements were made from samples prepared in an essentially CO<sub>2</sub>-free, H<sub>2</sub>O-free glove box and from samples prepared in ambient conditions. For those prepared in a CO<sub>2</sub>-free glove box, AFM imaging was conducted on (1) an unexposed air/coating surface, (2) an unexposed coating bulk, (3) an unexposed coating/substrate interface, and (4) a field exposed air/coating surface. For samples prepared in ambient conditions, only the unexposed air/coating surface was investigated. The same regions of the exposed samples were scanned periodically by the AFM to monitor changes in the surface morphology of the coating as UV exposure progressed. Small angle neutron scattering and Fourier transform infrared spectroscopy (FTIR) studies were performed to verify the microstructure and to follow chemical changes during outdoor exposure, respectively. The results have shown that amine blushing, which occurs only under ambient conditions, had a significant effect on the surface morphology and microstructure of the epoxy. The surface morphology of the samples prepared under CO<sub>2</sub>-free, dry conditions was generally smooth and homogeneous. However, the interface and the bulk samples clearly revealed a two-phase structure consisting of bright nodular domains and dark interstitial regions, indicating an inhomogeneous microstructure. Such heterogeneous structure of the bulk was in good agreement with results obtained by small angle neutron scattering of unexposed samples and by AFM phase imaging of the degraded sample surface. The relationship between submicrometer physical changes and molecular chemical degradation is discussed.*

*Keywords: Atomic force microscopy, surface analysis, epoxy resins, durability, physical properties, service life prediction, weatherability, surface chemistry*

Surface morphology and bulk microstructure play an important role in the physical and chemical degradation of an epoxy-based coating exposed to weathering environments. Although photochemical degradation of amine-cured epoxies has been extensively studied,<sup>1-5</sup> little research<sup>6,7</sup> has been focused on the physical degradation of these materials, particularly on morphological and microstructural changes at the early stage of degradation when the physical changes are only on submicrometer length scales. Additionally, the microstructure of amine-cured epoxies is still controversial, and this unresolved issue could hinder a complete understanding of degradation behavior of epoxies. A number of studies have reported that a thermoset epoxy network is inhomogeneous, containing high crosslink density regions from

6 nm to 10<sup>4</sup> nm in diameter and some low crosslinked interstitial regions.<sup>8-12</sup> On the other hand, several studies contend that the epoxies have a homogeneous microstructure.<sup>13-16</sup> One study suggested that the nodular structures often observed in the epoxy materials by electron microscopy are artifacts resulting from the interaction of the electron beam or etching agents with the sample surface.<sup>13-15</sup> Based on AFM analysis of the air/epoxy surface, a recent study also claimed that amine-cured epoxy has a homogeneous structure, similar to that of an amorphous thermoplastic.<sup>16</sup> Note that this study was based on the measurements taken only on the air/film surface, not from the bulk of the epoxy. Since the air surface of a polymeric film can have different chemical and physical properties than the bulk due to enrichment of

Presented at the 82nd Annual Meeting of the Federation of Societies for Coatings Technology, October 27-29, 2004, in Chicago, IL.

\* Building and Fire Research Laboratory, Gaithersburg, MD 20899.

† Gaithersburg, MD 20899.

\*\* Kansas City, MO 64110.



Figure 1—The chamber used for outdoor exposure, showing the exposure cells, the radiometer, and the wires connecting to the temperature and relative humidity sensors.

low surface-energy materials at the air surface,<sup>17-20</sup> further research is needed to verify whether the microstructure of the air surface can represent that of the bulk in an epoxy material.

In this study, AFM is used to study the surface morphology and bulk microstructure of an amine-cured epoxy before and after outdoor exposure. Atomic force microscopy (AFM) is a powerful technique that can provide direct spatial mapping of surface morphology with nanometer resolution. Further, the phase contrast in tapping mode AFM often reflects differences in the properties of individual components of heterogeneous materials, and is useful for compositional mapping in polymer blends and copolymers,<sup>21-26</sup> and heterogeneity mapping in polymer coatings.<sup>6,27,28</sup> Other advantages of AFM include minimal sample preparation procedure, operation in ambient condition, and a relatively nondestructive detection, making it suitable to use this technique to monitor the changes of the surface feature of the same sample as a function of exposure time. Samples studied in this article include the surface, interface, and microtomed fractured (bulk) specimens prepared in an essentially CO<sub>2</sub>-free, H<sub>2</sub>O-free glove box, and specimens prepared in ambient conditions. AFM studies of surface physical degradation were performed on specimens exposed outdoors. Small angle neutron scattering was also carried out to corroborate AFM results on the microstructure of the bulk, and FTIR transmission spectroscopy analysis was performed to provide chemical degradation information.

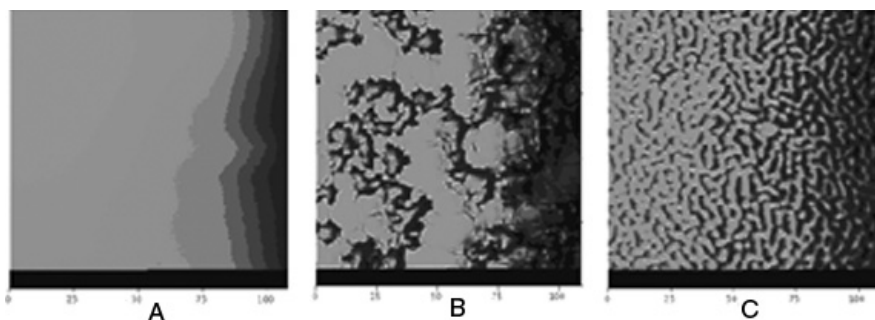


Figure 2—Optical images of the amine-cured epoxies prepared inside an essentially CO<sub>2</sub>-free, H<sub>2</sub>O-free glove box (A) and in ambient conditions (B and C). The approximate dimensions of the images are 110 μm × 110 μm.

## EXPERIMENTAL PROCEDURES\*

### Materials and Specimen Preparation

The amine-cured epoxy was a stoichiometric mixture of a pure diglycidyl ether of bisphenol A (DGEBA) with an epoxy equivalent of 172 g/equiv (DER 332, Dow Chemical) and 1,3-bis(aminomethyl)-cyclohexane (1,3 BAC, Aldrich). Appropriate amounts of toluene were added to the mixture, then all the components were mechanically mixed for seven minutes. After degassing in a vacuum oven at ambient temperature to remove most of the bubbles, the epoxy/curing agent/solvent mixture was applied to the substrates. Unless specified otherwise, all applications were carried out in an essentially CO<sub>2</sub>-free, dry glove box. Thick films used for microscopic imaging were approximately 150 μm in thickness and were obtained by casting the mixture onto silicon wafers using a drawdown technique. Thin films of approximately 7 μm thick used for transmission FTIR spectroscopy study were obtained by spin casting onto CaF<sub>2</sub> substrates at 209 rad/sec for 30 sec. Except for those used in the blushing study, all the samples were cured at room temperature for 24 hr in the CO<sub>2</sub>-free dry glove box, followed by heating at 130°C for two hours in an air-circulated oven. The glass transition temperature, T<sub>g</sub>, of the cured films was 123°C ± 2°C, as estimated by dynamic mechanical analysis.

The samples used for AFM microstructural studies of the interface were obtained by immersing the thick epoxy-coated silicon substrates in liquid nitrogen or hot water, followed by peeling the film away with tweezers. The film interior side that was in contact with the silicon substrate during film formation is termed the interface, and the side exposed to air is termed the surface. For study of the bulk microstructure, a thick film was microtomed by an ultra-fine microtomer.

### Outdoor UV Exposure

Outdoor UV exposures were carried out in Gaithersburg, MD. Specimens were first loaded into the multiple-window exposure cells which were then placed in an outdoor environmental chamber at 5° from the horizontal plane and facing south (Figure 1). The bottom of the chamber was made of black-anodized aluminum, the top was covered with borofloat glass, and all the sides were enclosed with a breathable fabric material that allowed water vapor, but prevented dust from entering the chamber. UV-visible spectral results showed that the borofloat glass did not alter the solar spectrum before or after more than one year of exposure in Gaithersburg. The specimen expo-

\*Certain commercial products or equipment are described in this article in order to specify adequately the experimental procedure. In no case does such identification imply recommendation or endorsement by the National Institute of Standards and Technology, nor does it imply that it is necessarily the best available for the purpose.

sure chamber was equipped with a thermocouple and a relative humidity sensor, and the temperature and relative humidity in the chamber were recorded once every minute, 24 hours per day for 365 days per year.

### Measurement Techniques

**ATOMIC FORCE MICROSCOPY (AFM)**—To image the morphology and microstructure of amine-cured epoxy coatings before and during outdoor exposures, a Dimension 3100 AFM (Digital Instruments) was used in tapping mode with commercial silicon probes from Veeco Metrology. The optical images were captured by the integrated optical microscope of the AFM. Topographic and phase images were obtained simultaneously using a resonance frequency of approximately 300 kHz for the probe oscillation and a free-oscillation amplitude of  $62 \text{ nm} \pm 2 \text{ nm}$ . The set-point ratio (the ratio of set point amplitude to the free amplitude) ranged from 0.60 to 0.80. Samples for AFM analysis included: (1) the surface, interface, and bulk specimens prepared inside the  $\text{CO}_2$ -free,  $\text{H}_2\text{O}$ -free glove box; (2) specimens applied and cured, but not mixed at ambient conditions outside of the glove box ( $22^\circ\text{C}$ , approximately 45% relative humidity); and (3) specimens exposed in the outdoor chamber at different times. For samples exposed outdoors, AFM measurements were performed at almost the same locations of the same sample to follow the structural changes of the same region with respect to the exposure time.

**FOURIER TRANSFORM INFRARED SPECTROSCOPY (FTIR)**—Chemical degradation of the epoxy coatings was measured by FTIR transmission using a PIKE autosampling accessory (PIKE Technologies), described previously.<sup>29</sup> This automated sampling device allowed efficient and rapid recording of the FTIR transmission spectra of the coating at all windows of the exposure cell before or after each exposure time. Since the exposure cell was mounted precisely on the autosampler, errors due to variation of sampling at different exposure times were essentially eliminated. The autosampler accessory was placed in an FTIR spectrometer compartment equipped with a liquid nitrogen-cooled mercury cadmium telluride (MCT) detector. Spectra were recorded at a resolution of  $4 \text{ cm}^{-1}$  and 128 scans. The peak height was used to represent IR intensity, which is expressed in absorbance. All FTIR results were the average of four specimens.

**SMALL ANGLE NEUTRON SCATTERING (SANS)**—SANS experiments over  $q$  (wave vector) range from  $0.009 \text{ \AA}^{-1}$  to  $0.138 \text{ \AA}^{-1}$  were carried out using the eight-meter SANS instrument at the National Institute of Standards and Technology (NIST) Center for Neutron Research. The incident neutron wavelength was  $\lambda = 8 \text{ \AA}$  with a wavelength

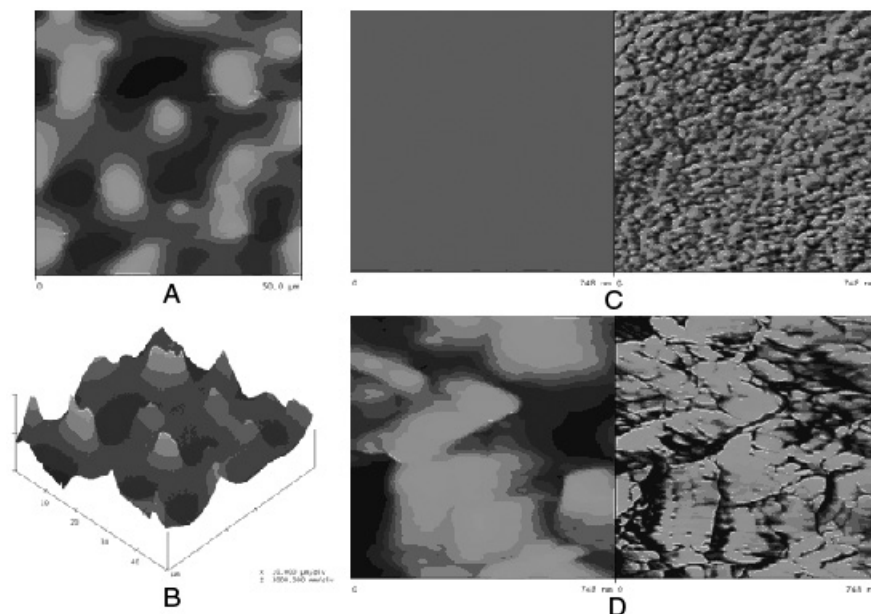


Figure 3—2D AFM height image (A) and corresponding 3D height image (B) of amine-cured epoxy prepared in ambient conditions. Scan size is  $50 \mu\text{m} \times 50 \mu\text{m}$ , and the height scale from white to black is  $3 \mu\text{m}$ . (C) and (D) are AFM height and phase images obtained from the “valley” and the “hill” of image B, respectively, at high magnification. Scan size is  $0.748 \mu\text{m} \times 0.748 \mu\text{m}$ , and the contrast variations from white to black are  $150 \text{ nm}$  for the height images and  $30^\circ$  for the phase images.

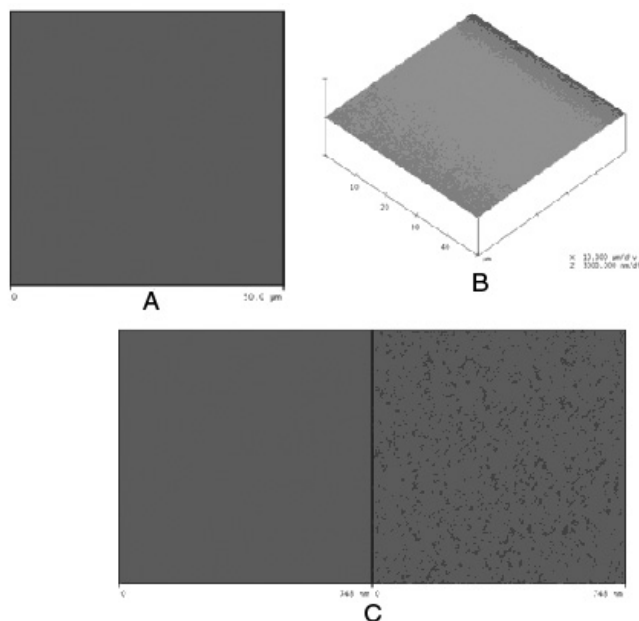


Figure 4—AFM 2D height image (A) and corresponding 3D height image (B) of amine-cured epoxy cured in an essentially  $\text{CO}_2$ -free,  $\text{H}_2\text{O}$ -free glove box. Scan size is  $50 \mu\text{m} \times 50 \mu\text{m}$ , and the height scale from white to black is  $3 \mu\text{m}$ . (C) shows AFM height and phase images obtained from one  $0.748 \mu\text{m} \times 0.748 \mu\text{m}$  region of image A. The contrast variations from white to black are  $150 \text{ nm}$  for the height images and  $30^\circ$  for the phase images.

resolution of  $\Delta\lambda/\lambda = 0.15$ . The scattered intensity was corrected for background and parasitic scattering, placed on an absolute level using a calibrated secondary standard and circularly averaged to yield the scattered intensity,  $I(q)$ , as a function of the wave vector,  $q$ , where  $q = (4\pi/\lambda) \sin(\theta/2)$  ( $\theta$  is the scattering angle).



## RESULTS AND DISCUSSION

### Surface Microstructure and Amine Blushing

Amine-cured epoxy materials often show surface whitening, low gloss patches, or oiliness if the curing occurs under conditions of cool ambient temperatures or high humidity. This phenomenon is commonly known as “amine blushing” or “blushing.”<sup>30</sup> Generally, blushing is caused by sorption of moisture and carbon dioxide from the atmosphere during curing. The solvent in the coating could make blushing more pronounced because the evaporation of the solvent can cause the temperature of the applied film to fall below the dew point of the water-laden air, resulting in condensation of water on the coating surface.<sup>31</sup> For small molecular-mass primary amines, such as 1,3-bis(aminomethyl)-cyclohexane (1,3 BAC) used in this study, the reaction between amines and carbon dioxide is rapid, and the addition of moisture increases the sorption

capacity and the reaction rate.<sup>30</sup> To eliminate blushing, several strategies have been recommended, such as lowering the amine concentration, decreasing gel times, improving the resin/amine compatibility, or processing under a controlled condition. In this study, the blushing was minimized by preparing and initially curing the samples in an essentially CO<sub>2</sub>-free, H<sub>2</sub>O-free glove box. Figure 2 shows optical microscopic images of the films prepared inside the controlled glove box (A) and at laboratory ambient conditions (B and C). Except for a few particles, the surfaces of samples prepared in the CO<sub>2</sub>-free glove box are smooth within the 110 μm × 110 μm imaging areas. However, for those prepared in ambient laboratory conditions, the sample surfaces are cloudy and not as glossy. The white clusters, patches, and particles (Figure 2B) and well-organized patterned features (Figure 2C) are commonly observed with this amine-cured epoxy system. The organized pattern is similar to the so-called bicontinuous spinodal decomposition structures, which are usually found during the phase separation in the systems of multi-components.<sup>32,33</sup> Spinodal decomposition usually forms because the mixture is unstable due to infinitesimal fluctuations in density or composition and thus separates spontaneously into two phases.<sup>32</sup> The reason for such phenomenon in the present epoxy system is not clear. The presence of moisture in the air may change the solvent evaporation rate and the reactions between CO<sub>2</sub> and amine curing agent. Both of these effects may cause a phase separation in the film surface while the epoxy resin is reacting with the amine curing agent during curing in ambient conditions.

Additional morphological and microstructural information for samples prepared in ambient conditions can be found in Figure 3. In this figure, A and B are the 2D and 3D AFM height images, respectively, in a 50 μm × 50 μm scanning area, and C and D are the 2D height and phase images from the “hill” and the “valley” in part B with a scanning area of 0.748 μm × 0.748 μm. For comparison, AFM images of the samples prepared inside the glove box are displayed in Figure 4. Figure 3 shows that samples prepared in ambient conditions have a rougher surface than those prepared in the essentially CO<sub>2</sub>-free dry environment. A substantial difference in the microstructure between the “hill” and the “valley” regions can also be seen in the ambient-prepared samples. The “valley” region is relatively smooth, having features that are quite similar to those of the entire surface of samples prepared in the glove box. On the other hand, the “hill” region consists of many crystal-like structures that exhibit certain orientations. These “hills” are possibly composed of mostly the salts of carbamate zwitterions or ammonium bicarbonate, which are the reaction products between CO<sub>2</sub> of the air and amine curing agent.<sup>30</sup> Characterization of the surface chemical heterogeneity of these samples is being investigated. From the above results, it is clear that blushing does greatly alter the morphology and the microstructure of an amine-cured coating surface. Such change will have an effect on the appearance, wettability, surface physical degradation, and sorption of water on amine-cured coatings. One can also find that blushing in the epoxy system used in this study can be successfully minimized by preparing samples in an essentially CO<sub>2</sub>-free, H<sub>2</sub>O-free environment.

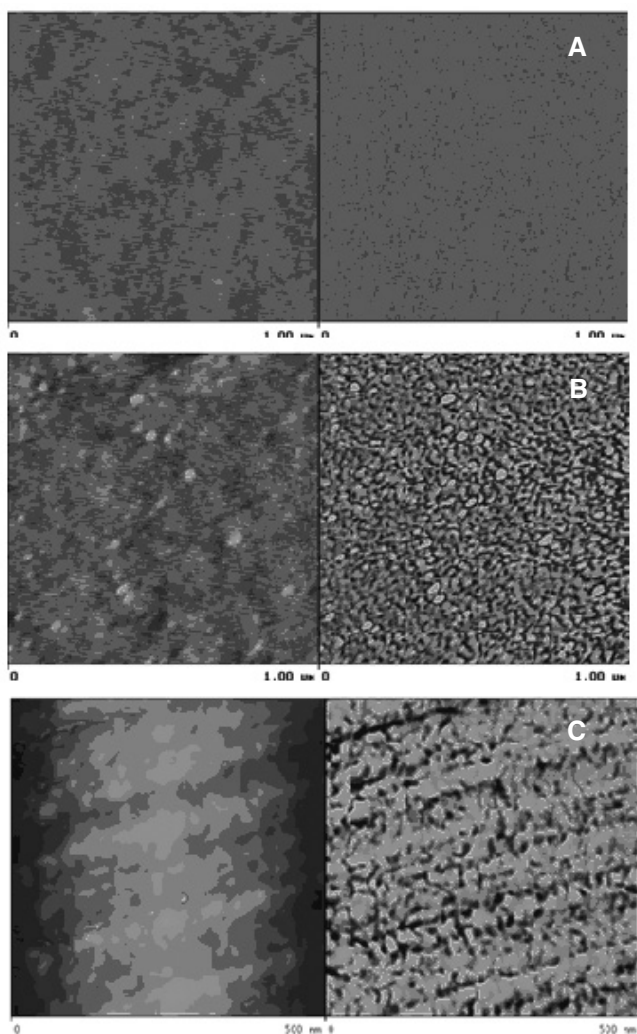


Figure 5—AFM height images (left) and phase images (right) of epoxy coatings: (A) surface, (B) interface, and (C) bulk samples. Scan size is 1 μm × 1 μm for (A) and (B), 500 nm × 500 nm for (C). Contrast variations in (A) and (B) from white to black are 10 nm for the height images and 90° for the phase images; in (C) from white to black are 10 nm for the height images and 30° for the phase image.

### Surface, Interface, and Bulk Microstructures of Epoxy

AFM height and phase images of the surface, interface, and bulk samples are presented in *Figure 5*. The surface sample appeared homogeneous and smooth with little phase contrast. On the other hand, the interface sample was rougher, showing a two-phase microstructure consisting of a light matrix and relatively dark interstitial regions in the phase image. It should be mentioned that the silicon surface, where the interface samples were initially in contact and from which they were peeled, was essentially smooth and featureless, as observed in AFM images with the same magnification (not shown). *Figure 5C* displays the microstructure obtained from an ultramicrotomed fractured surface of a bulk sample. Although these images are not distinct (probably due to the microtoming action), and the nodular structures are not as organized as those of the interface sample, *Figure 5C* does show a similar inhomogeneous feature as that of the interface. Such a heterogeneous microstructure is consistent with those observed for other epoxies<sup>28,34,35</sup> and an acrylic-melamine coating interface.<sup>36</sup> Further, the difference in the microstructure between the surface and the interface has been observed in other amine-cured epoxies and other polymeric coatings.<sup>35,37</sup> It is suggested that the outermost surface layer of an amine-cured epoxy is homogeneous; however, the microstructure of the bulk and the interface is heterogeneous. Although the contrast mechanism in phase imaging is not fully understood, for moderate tapping force, the bright regions in the phase image usually correspond to harder materials and the darker-phased regions to more compliant materials.<sup>23,24</sup> It is reasonable to conclude that the bulk microstructure of an amine-cured epoxy is heterogeneous, consisting of softer regions dispersed in a harder matrix. The harder, nodular domain in the matrix has been attributed to highly crosslinked material and the soft interstitial regions to less crosslinked, low molecular mass material.<sup>8,11,28</sup> The high crosslink density regions have been reported to be only weakly attached to the surrounding matrix,<sup>10,11</sup> and their size varies with cure process and other conditions.<sup>10</sup>

A previous AFM study also reported that the air surface of an amine-cured epoxy is homogeneous.<sup>16</sup> Based on this observation, the authors have concluded that the epoxy-amine networks are homogeneous at the nanometer scale. This observation is consistent with our results in *Figure 5A*, which show that the air surface is homogeneous, with smooth topography and little phase contrast. However, both the interface and the bulk microstructures exhibited substantially more topographic and phase contrast than that of the surface (*Figures 5B* and *5C*). The homogeneous structure of the air surface is believed to be due to an enrichment of low surface energy materials at the air-film surface. Our previous results on contact angle measurements and surface-free energies of several amine-cured systems have shown that the air surface has a lower polarity than that of the interface, providing a good argument for such a hypothesis.<sup>34</sup> Further, enrichment of a low surface-free energy material at the air surface is a common phenomenon in multiple component systems.<sup>17-20</sup> The presence of this homogeneous, enriched outermost layer probably would mask the bulk microstructure under-

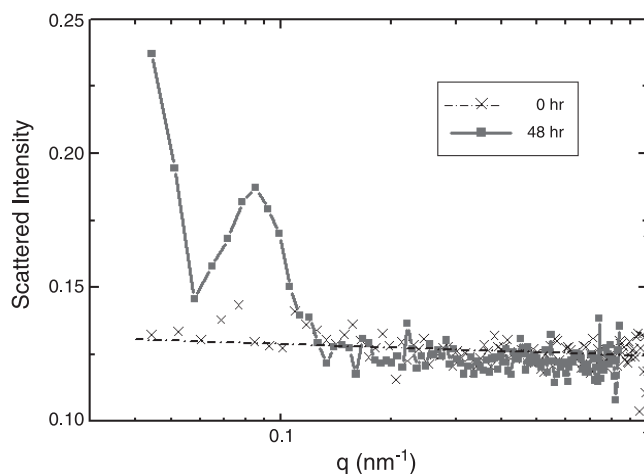


Figure 6—Small angle neutron scattering curves of epoxy film soaked in deuterated acetone for 0 hr (---) and 48 hr (—). The estimated extended uncertainties ( $k=2$ ) in the SANS data presented in this paper are smaller than the size of symbols in all figures.

neath. Therefore, the inhomogeneous structure observed in *Figures 5B* and *5C* is believed to be the inherent structure of this amine-cured epoxy. It is noted that, even though the topography could bring about the artifacts of the phase images in some cases, the independence of the phase contrast on the height image shown in *Figures 5B* and *5C* suggest that the phase contrast in *Figure 5* is not due to the topography, but more likely due to the property difference of the multiple components in the network.

To validate the heterogeneous microstructure of this epoxy, SANS measurements were performed on the same epoxy before and after soaking with deuterated acetone (d-acetone). In principle, if the epoxy network is homogeneous on a nanometer scale, even after soaking in d-acetone, only the incoherent neutron scattering would be observed. On the other hand, in a heterogeneous network, the neutron scattering curves would be expected to deviate from the incoherent background when the inhomogeneous structures are swollen and the neutron contrast would be enhanced by d-acetone. *Figure 6* shows the results of SANS study. For dry bulk samples, only incoherent scattering background was observed, and there was no visible neutron contrast. After soaking in d-acetone for 48 hr, however, an obvious peak appeared at  $q = 0.008517 \text{ nm}^{-1}$ , and an upturn had been observed in relatively low  $q$  region (ca.  $q < 0.03 \text{ \AA}^{-1}$ ). The enhanced neutron intensity is due to the diffusion of d-acetone into the epoxy film, where a lower crosslink density region tends to absorb more d-acetone than a higher crosslink density region; therefore, the neutron contrast between these two regions is increased by the sorption of d-acetone. The peak indicated the existence of a correlated microdomain structure. The value of the peak position can be related to an average d-spacing ( $d=2\pi/q$ ) between the microdomains, which is approximately 74 nm. This value is consistent with the size of nodules obtained from the AFM, especially when the swollen effect is taken into account. The upturn in the relatively low  $q$  region suggests that a correlation length between the domains exists on a larger length scale. The multiple features of the scattering



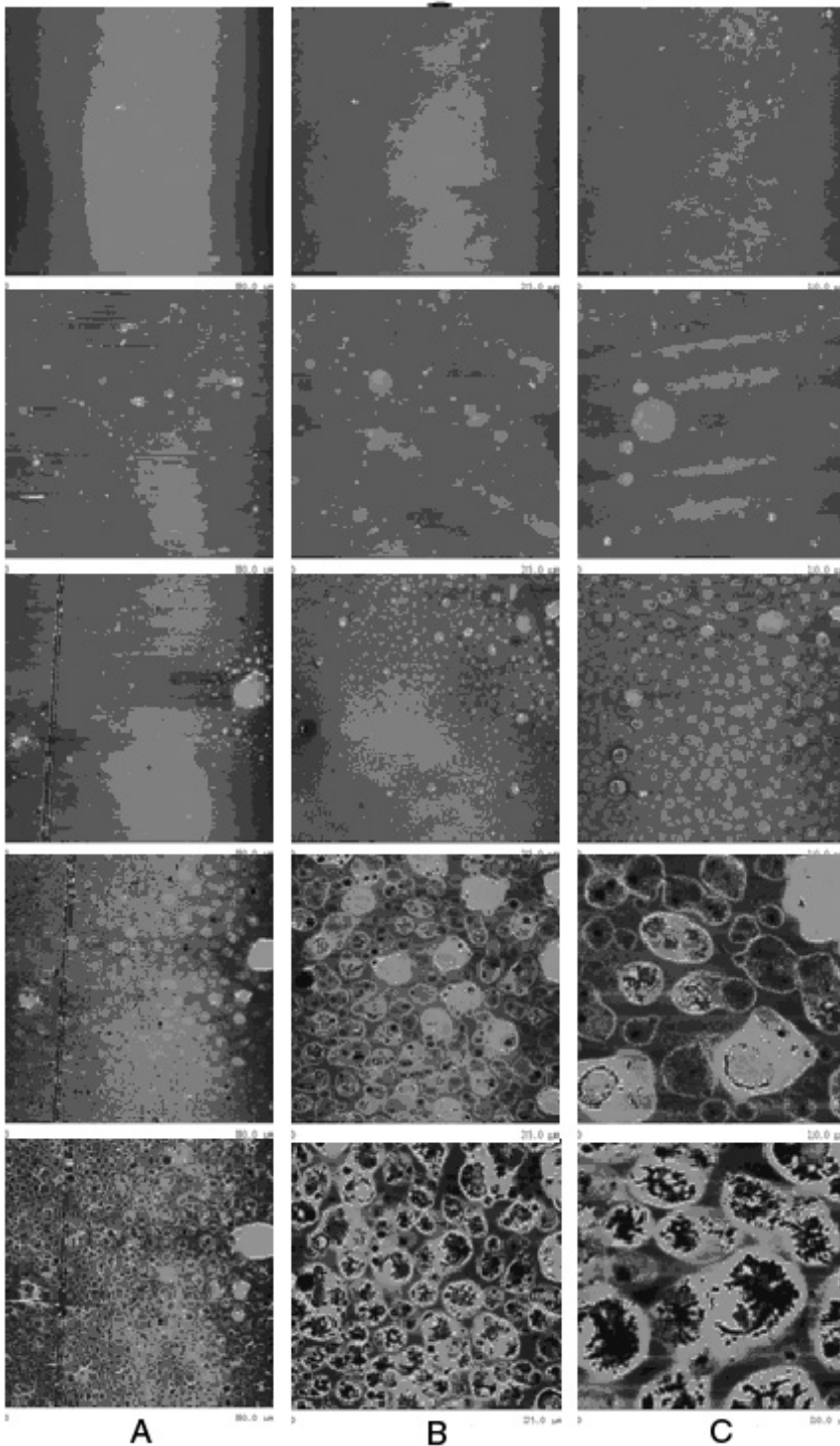


Figure 7—AFM topographic images of the epoxy coating after exposure to outdoors during March and June for (from top to bottom) (6, 38, 69, 77 and 84) days. Lateral dimensions for the images in A column is  $80\ \mu\text{m} \times 80\ \mu\text{m}$ ; in B column is  $25\ \mu\text{m} \times 25\ \mu\text{m}$ ; in C column is  $10\ \mu\text{m} \times 10\ \mu\text{m}$ . The height scales from white to black for A, B, and C are 100 nm, 50 nm and 25 nm, respectively.

curve could be due to a broad domain size distribution or the existence of some irregularly packed structures. The above SANS data are consistent with the heterogeneous microstructures observed by AFM, suggesting that the heterogeneous nodular structures not only exist on the interface side of the sample, but also inherently exist

through the bulk of the epoxy. Such a heterogeneous structure is confirmed further with the microstructure of the degraded sample, which will be shown later. It is believed that the lower crosslink density regions, unreacted and partially reacted materials in the heterogeneous structure, would have an influence on the degradation behavior of an amine-cured epoxy material.

### ***Morphological and Microstructural Changes of Epoxy after UV Exposure***

AFM topographic images of the epoxy coating after exposure to an outdoor environment chamber in Gaithersburg, MD are shown in Figure 7. Approximately the same regions of the specimen were measured with exposure time. From top to bottom in Figure 7, the exposure times are 6, 38, 69, 77, and 84 days, respectively. Three scan sizes,  $80\ \mu\text{m} \times 80\ \mu\text{m}$ ,  $25\ \mu\text{m} \times 25\ \mu\text{m}$ , and  $10\ \mu\text{m} \times 10\ \mu\text{m}$ , are presented as columns A, B, and C. Typically, a smaller scanning dimension was selected from a fixed location of a larger frame; thus, the degradation of the same region of the sample was followed in all scan sizes. General microscale morphological changes due to degradation can be observed from the  $80\text{-}\mu\text{m}$  scan size. However, detailed microstructural changes can be better seen with the high magnification in the smaller scan sizes. Figure 8 displays the corresponding 3D AFM topographic images of Figure 7 with a  $5\ \mu\text{m} \times 5\ \mu\text{m}$  scanning area. For the first six days of exposure, the surface was similar to that of the unexposed samples, which was smooth with a few small protuberances (bright spots) that might be due to defects resulting from the sample preparation. After 38 days, a few circular features started to appear, which can be seen clearly in the  $10\ \mu\text{m} \times 10\ \mu\text{m}$  scan. The 3D images of Figure 8 show that these circular features are protuberances varying in sizes. After 69 days of exposure, some protuberances seemed to disappear, and some became smaller, but a pronounced structure appeared in some locations of the surface, surrounded by many new circular features. From higher magnifications and 3D presentation, those new features were observed as well-distributed pits (Figure 8C). These pits, having the elevated edges, average about  $0.3\ \mu\text{m}$  in diameter. The three relatively large pits in Figure 8C are believed to be the original three obvious protuberances

shown in Figure 8B. More degradation features appeared after 77 days and almost covered the entire 80  $\mu\text{m}$ -scanned area. These features are generally organized and larger but not as circular as at shorter exposure times. It could be because the previously formed smaller pits have coalesced to form large pits whose depths also increase with time. The enlargement and the deepening of those degradation pits became more severe as the degradation progressed. After 84 days of exposure, the surface was dominated by the coalesced deep pits. The elevated edges of those pits were still obvious at this stage, exhibiting a rough topography. The above microscopic results are consistent with the gloss measurements on these samples, which showed a substantial loss of gloss after 84 days of exposure (not shown). Additionally, it is important to note that the degradation features observed above have reproducibly been observed for this amine-cured epoxy exposed to outdoors, regardless of the month the exposure began, film thickness, or substrates used. The origin of these features is still under investigation.

A high-resolution AFM imaging was performed on a 1  $\mu\text{m} \times 1 \mu\text{m}$  region where several circular pits were observed (Figure 9). The phase images of the pitted regions clearly show a two-phase microstructure similar to those observed from the interface and microtomed samples (Figure 3). The bright nodules in the two-phase microstructure appear larger than those observed in the interface or in the bulk, and they grow in size as the pit enlarges with exposure time. Further studies are needed to establish whether the observed microstructure is due to the inherently heterogeneity of the epoxy or if it is formed during degradation. Nevertheless, the two-phase microstructure observed in the degraded pits probably gives an additional evidence for the existence of inherently heterogeneous structure in the bulk of the epoxy. Because of the similarity in the observed microstructure between the bulk and the degraded surface, however, we believe that the degradation of the outermost layer exposes the bulk microstructure. Further, the degradation-susceptible regions (low molecular mass, low crosslink density regions) in the two-phase domains undergo degradation first, resulting in a modified microstructure observed inside the pits.

To relate the morphological changes to the chemical degradation of this amine-cured epoxy coating, FTIR measurements were performed on the 7  $\mu\text{m}$ -thick spin-cast films on  $\text{CaF}_2$  at different exposure times. These results are presented in Figure 9. The difference spectra were obtained by subtracting the spectrum of the unexposed sample from that of the exposed one after adjusting for any baseline shift. Three exposure times close to those used in the AFM study are shown. The bands of interest for studying the degradation of an amine-cured epoxy coating are those at 1250  $\text{cm}^{-1}$ , 1510  $\text{cm}^{-1}$ , 1658  $\text{cm}^{-1}$ , 1728  $\text{cm}^{-1}$ , 2925  $\text{cm}^{-1}$ , and 3400  $\text{cm}^{-1}$ . The 1250  $\text{cm}^{-1}$  band is

attributed to C–O stretching of aryl ether, 1510  $\text{cm}^{-1}$  to benzene ring stretching, and 2925  $\text{cm}^{-1}$  to  $\text{CH}_2$  antisymmetric stretching. The decrease in intensities of these bands indicates that chain scission and mass loss in the films have taken place. In addition to the intensity decreases of the existing bands, the spectra show the formation of new chemical species in the 1620  $\text{cm}^{-1}$  to 1800  $\text{cm}^{-1}$  region as a result of exposures. Two prominent bands at 1658  $\text{cm}^{-1}$  and 1728  $\text{cm}^{-1}$ , which are assigned to C=O stretching of a ketone and amide C=O stretching, respectively, are due to formation of oxidation products. The OH stretching bands near 3400  $\text{cm}^{-1}$  also shift to lower frequency and new bands appear around 3225  $\text{cm}^{-1}$ . The above FTIR results are in good agreement with the photooxidative mechanisms proposed by Bellinger and Verdu<sup>2-4</sup> for epoxy cured with aliphatic amines.

The plots of FTIR absorbance for the amide C=O stretching band at 1658  $\text{cm}^{-1}$  and the aromatic ring stretching band at 1510  $\text{cm}^{-1}$  as a function of exposure time are shown in Figure 10. Each data point in this figure was the average of four specimens. The standard deviation of the four samples is less than  $\pm 10\%$  of the average value. A, B, C, D, and E pointing to 6, 38, 69, 77, and 84 days of exposure correspond to the five exposure times shown in

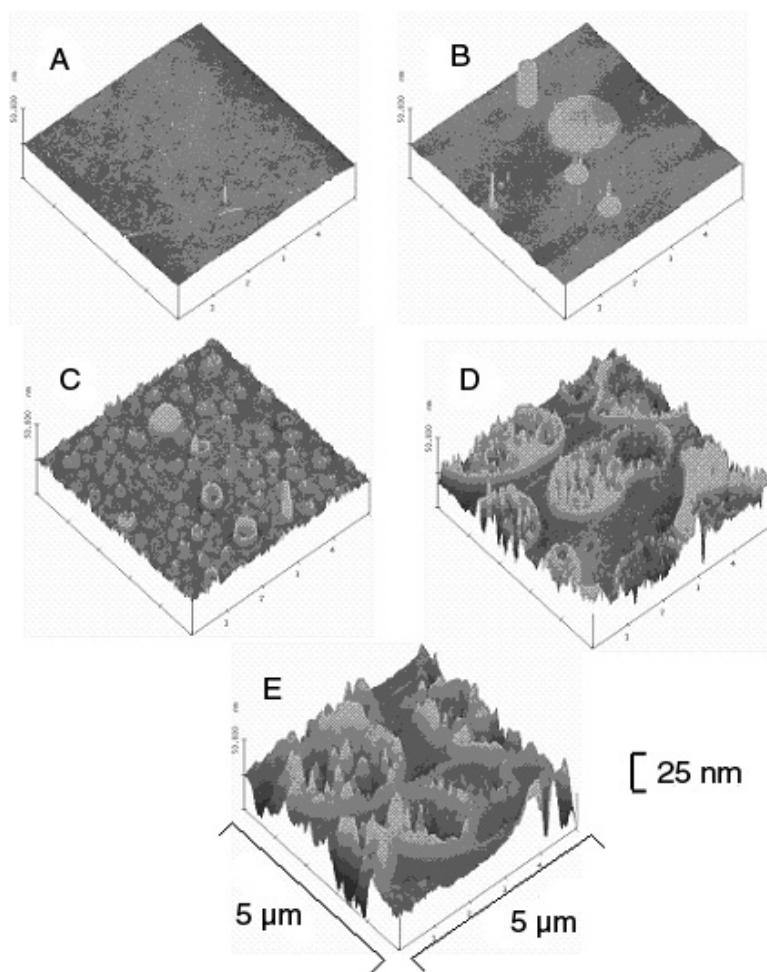


Figure 8—3D AFM topographic images of the epoxy coating after exposure to outdoors during March and June for (A) 6 days, (B) 38 days, (C) 69 days, (D) 77 days, (E) 84 days. Lateral dimension for the images is 5  $\mu\text{m} \times 5 \mu\text{m}$ . The height scale is 25 nm.



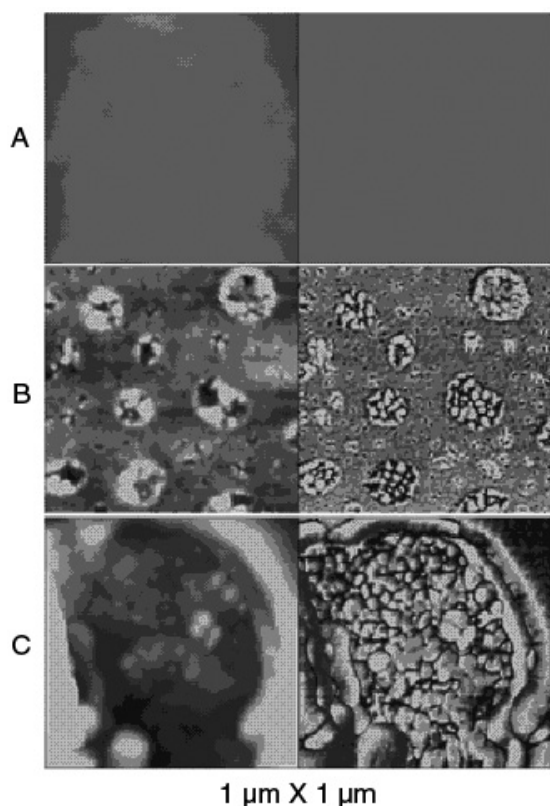


Figure 9—AFM height (left) and phase (right) images of the epoxy exposed to outdoors during May and July: (A) before exposure, (B) after exposure for 1 month, and (C) after exposure for 2 months. The scan size is  $1\ \mu\text{m} \times 1\ \mu\text{m}$ . Contrast variation from black to white is 30 nm for height image and  $60^\circ$  for phase image.

Figures 7 and 8 in the AFM study. The decrease of the  $1510\ \text{cm}^{-1}$  band intensity was nearly linear with exposure time. On the other hand, the amide formation at  $1658\ \text{cm}^{-1}$  reached a maximum after approximately 80 days and appeared to decrease after 90 days of exposure. The decrease in the FTIR intensity of the oxidation products at long exposures was probably due to a combination of a depletion of the degradable materials and the loss (both physical and chemical) of the oxidation products.<sup>38</sup>

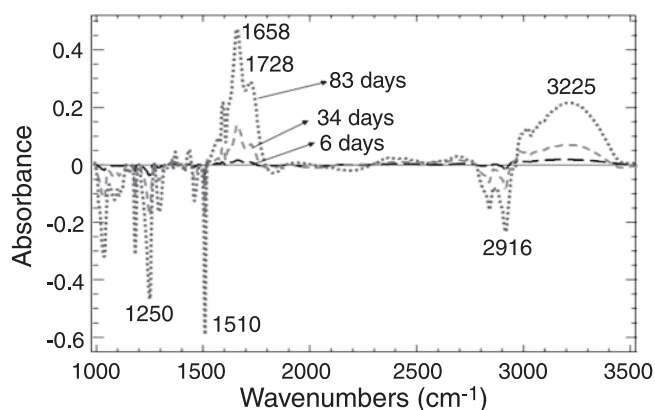
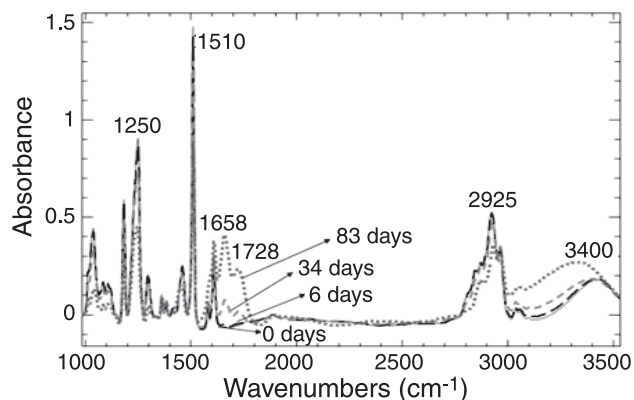


Figure 10—FTIR spectra of the amine-cured epoxy after exposure to outdoors during March and June for 0 (—), 6 (---), 34 (- - -) and 83 (....) days: (left) absorbance spectra; (right) difference spectra.

A relation may be established between the nanoscale physical changes shown in Figures 7 and 8 and the chemical degradation presented in Figure 11. Chemical degradation processes such as oxidation, chain scission, and mass loss are likely the origins of surface morphological changes observed by AFM. The migration of oxidation products may also happen during deepening and enlargement of the pits. The rates of these processes depend strongly on the availability of the reactants, i.e., oxygen and the degradable chemical species in the film. It should be noted that the oxidation reactions can only take place when oxygen is available, and the rate of oxidation product formation should be greater at locations where oxygen is more abundant. However, it is unknown why the protuberances have a regular pattern and the initial pit distribution is so uniform. Nanoscale physical and chemical measurements are needed to provide a good understanding of these degradation behaviors.

Physical changes monitored by the AFM appeared to follow qualitatively with chemical degradation reasonably well for an amine-cured epoxy exposed to outdoors. For example, for the first six days of exposure, FTIR results exhibited a small but detectable chemical change (letter A, Figure 11). The corresponding AFM images show no visible features, but the surface root mean square roughness results obtained from the AFM images during this period revealed a roughness increase, indicating that the surface morphology and microstructure had been changed. On further exposure, when the surface topographic changes were severe, a substantial chemical degradation had also occurred. For example, when the surface was dominated by the circular pits at 77 days of exposure, amide formation almost reached a near maximum and benzene ring loss was approximately 35%. Therefore, nanoscale imaging of degradation by an AFM can be helpful to establish a relationship between physical and chemical degradation of polymer coatings during UV exposure, particularly at the early stages of degradation when physical changes are on a submicrometer length scale.

## SUMMARY

AFM was used to study the surface morphology and microstructure of an amine-cured epoxy before and after ex-



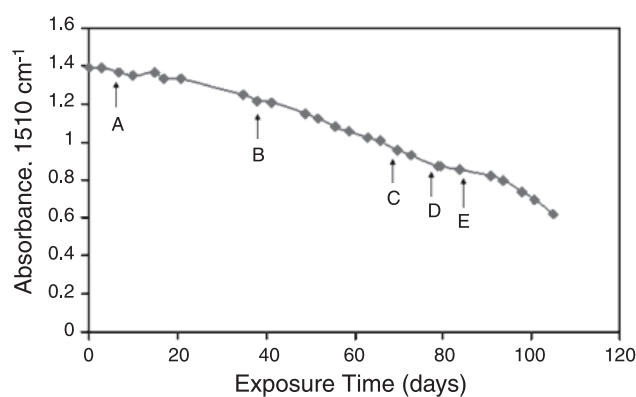
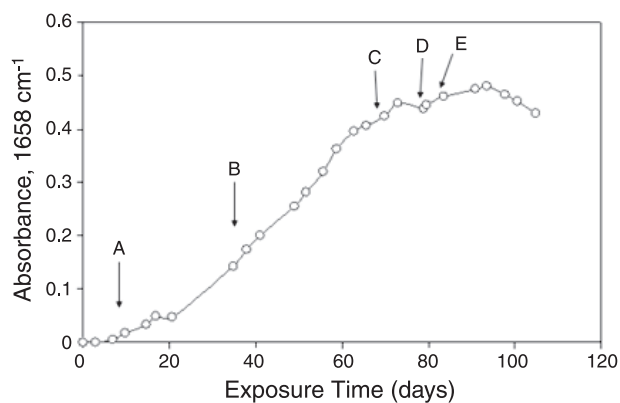


Figure 11—Plots of FTIR intensity for amide C=O stretching band ( $1658\text{ cm}^{-1}$ ) and aromatic ring stretching band ( $1510\text{ cm}^{-1}$ ) as a function of time of exposure to outdoors during March and June. The letters of A, B, C, D, and E correspond to (6, 38, 69, 77, and 84) days of exposure, respectively. Each data point in this figure was the average of four specimens. The standard deviation of the four samples was within  $\pm 10\%$  of the average value.

posures to outdoors. When samples were prepared inside an essentially  $\text{CO}_2$ -free and  $\text{H}_2\text{O}$ -free environment, a featureless, smooth surface was observed. However, AFM results of samples prepared at ambient conditions revealed a patchy appearance (blushing) or patterned surface morphology resembling a spinodal decomposition structure. The interface and bulk microstructures showed a two-phase structure consisting of bright nodular domains with dark interstitial regions in the AFM phase images. Such heterogeneous microstructure of the bulk is consistent with small angle neutron scattering results, which show an obvious peak and an upturn in the low  $q$  region of the scattering profile, indicating clearly a heterogeneous microstructure of this epoxy material. This two-phase heterogeneous structure was also observed on degraded sample surfaces.

AFM was used to follow morphological and microstructural changes of the epoxy during outdoor exposure. The same fixed locations on the samples were measured with exposure times. The formation of spotty protuberances was observed at the early degradation stages, followed by the appearance of circular pits having different sizes as exposure continued. At long exposure times, the circular features enlarged and deepened, resulting in a rough surface topography. FTIR analyses revealed substantial chemical degradation, with the formation of various oxidation products and mass loss of various chemical groups in the films after exposure to outdoors. These chemical processes are likely the main reason for surface morphological changes observed by AFM, and a qualitative relation between nanoscale physical changes and chemical degradation was observed. In summary, AFM is a powerful technique to study surface, bulk, and interface microstructure of an amine-cured epoxy. It also provides nanoscale information essential for linking physical changes and chemical degradation of polymeric coatings during outdoor exposure.

## ACKNOWLEDGMENTS

This research is part of a Government/Industry consortium on Service Life Prediction of Coatings at NIST. Companies involved in this consortium include Akzo Nobel Inc., ATOFINA, Atlas Electric Devices Inc., Dow Chemical Company, and The Sherwin-Williams Co. The Federal Highway Administration, Wright Patterson AFB,

and Forest Products Laboratory also provided additional funds for this research. We thank the Dow Chemical Company for providing the epoxy resin. We also acknowledge the support of the National Institute of Standards and Technology, and the U.S. Department of Commerce for providing the neutron research facilities used in this work.

## References

- (1) Rabek, J.F., *Polymer Photodegradation—Mechanisms and Experimental Methods*, Chapman & Hall, New York, pp 269-278, 1995.
- (2) Bellinger, V., Bouchard, C., Claveirolle, P., and Verdu, J., "Photo-oxidation of Epoxy Resins Cured by Non-Aromatic Amines," *Polym. Photochemistry*, 1, 69 (1981).
- (3) Bellinger, V. and Verdu, J., "Oxidative Skeleton Breaking in Epoxy-Amine Networks," *J. Appl. Polym. Sci.*, 30, 363 (1985).
- (4) Bellinger, V. and Verdu, J., "Structure-Photooxidative Stability Relationship of Amine-Crosslinked Epoxies," *Polym. Photochemistry*, 5, 295-311 (1984).
- (5) Monney, L., Belali, R., Vebrel, J., Dubois, C., and Chambaudet, A., "Photochemical Degradation Study of an Epoxy Material by IR-ATR Spectroscopy," *Polym. Degrad. Stab.*, 62, 353-359 (1998).
- (6) Nguyen, T., Gu, X., VanLandingham, M.R., Rytz, R., Nguyen, D., and Martin, J.W., "Nanoscale Characterization of Coatings Surface Degradation with Tapping Mode AFM," *Proc. Adhesion Society Meeting*, Anderson, G.L. (Ed.), p. 505, 2003.
- (7) Nguyen, T., Gu, X., VanLandingham, M.R., Byrd, E., Martin, D., Rytz, R., and Martin, J.W., "Degradation Modes of Polymeric Coatings Exposed to UV," *Proc. Coatings for Plastics Symposium*, Troy, MI, July, 2004.
- (8) Morgan, R.J. and O'Neal, J.E., "The Durability of Epoxies," *Polym.-Plast. Technol. Eng.*, 10, 49-116 (1978).
- (9) Kenyon, A.S. and Nielsen, L.E., *J. Macromol. Sci., Chem.*, A3 (2), 275 (1969).
- (10) Erath, E.H. and Robinson, M., *J. Polym. Sci., Part C*, 3, 65 (1963).
- (11) Cuthrell, R.E., "Epoxy Polymers. II. Macrostructure," *J. Appl. Polym. Sci.*, 12, 1263 (1968).
- (12) Karyakina M.V., Mogilevich, M.M., Maiorova, N.V., and Udalova, A.V., "Structure Formation Processes at Stages Preceding Formation of Network Polymers," *Vysokomol. Soedin.*, A17, 466-470 (1975).
- (13) Dusek, K., "Are Cured Thermoset Resins Inhomogeneous?," *Angewandte Makromol. Chem.*, 240, 1-15 (1996).
- (14) Dusek, K., Plestil, J., Lednický, F., and Lunak, S., "Are Cured Epoxy-Resins Inhomogeneous?," *Polymer*, 19, 393-397 (1978).
- (15) Oberlin, A., Ayache, J., Oberlin, M., and Guigon, M., "High-Resolution Dark-Field Imaging in Epoxy and Polyimide Systems," *J. Polym. Sci., Polym. Phys.*, Ed. 20, 579-591 (1982).
- (16) Duchet, J. and Pascault, J.P., "Do Epoxy-Amine Networks Become Inhomogeneous at the Nanometric Scale?," *J. Polym. Sci. Polym. Phys.*, Ed. 41, 2422-2432 (2003).

- (17) Thomas, H.R. and Omalley, J.J., "Surface Studies on Multicomponent Polymer Systems by X-ray Photoelectron-Spectroscopy-Polystyrene-Poly(ethylene oxide) Diblock Copolymers," *Macromolecules*, 12, 323-329 (1979).
- (18) Lee, W.K., Cho, W.J., Ha, C.S., Takahara, A., and Kajiyama, T. "Surface Enrichment of the Solution-Cast Poly (methyl methacrylate) Poly (vinyl acetate) Blends," *Polymer*, 36, 1229-1234 (1995).
- (19) Ebbens, S.J. and Badyal, J.P.S., "Surface Enrichment of Fluorochemical-Doped Polypropylene Films," *Langmuir*, 17, 4050-4055 (2001).
- (20) Chen, X., McGurk, S.L., Davies, M.C., Roberts, C.J., Shakesheff, K.M., Tendler, S.J., and Williams, P.M., "Chemical and Morphological Analysis of Surface Enrichment in a Biodegradable Polymer Blend by Phase-Detection Imaging Atomic Force Microscopy," *Macromolecules*, 31, 2278-2283 (1998).
- (21) Cleveland, J.P., Anczykowski, B., Schmid, A.E., and Elings, V.B., "Energy Dissipation in Tapping-Mode Atomic Force Microscopy," *Appl. Phys. Lett.*, 72, 2613-2615 (1998).
- (22) Magonov, S.N. and Reneker, D.H., "Characterization of Polymer Surfaces with Atomic Force Microscopy," *Annu. Rev. Mater. Sci.*, 27, 175-222 (1997).
- (23) Magonov, S.N., Elings V., Whangbo, M.H., "Phase Imaging and Stiffness in Tapping-Mode Atomic Force Microscopy," *Surf. Sci.*, 375, L385-L391 (1997).
- (24) Bar, G., Thomann Y., and Whangbo, M.H., "Characterization of Morphologies and Nanostructures of Blends of Poly(styrene) Block-Poly(ethane-co-but-1-ene)-Block-Poly(styrene) with Isotactic and Atactic Polypropylenes by Tapping-Mode Atomic Force Microscopy," *Langmuir*, 14, 1219-1226 (1998).
- (25) Raghavan, D., Gu, X., Nguyen, T. VanLandingham, M.R., and Karim, A., "Mapping Polymer Heterogeneity Using Atomic Force Microscopy Phase Imaging and Nanoscale Indentation," *Macromolecules* 33, 2573-2583 (2000).
- (26) Raghavan, D., Gu, X., Nguyen, T. and VanLandingham, M.R., "Characterization of Chemical Heterogeneity in Polymer System Using Hydrolysis and Tapping-Mode Atomic Force Microscopy," *J. Polym. Sci., Polym. Phys.*, 39, 1460-1470 (2001).
- (27) Gu, X., Raghavan, D., Nguyen, T., and VanLandingham, M.R., "Characterization of Polyester Degradation Using Tapping Mode Atomic Force Microscopy: Exposure to Alkaline Solution at Room Temperature," *Polym. Degrad. Stab.*, 74, 139-149 (2001).
- (28) VanLandingham, M.R., Eduljee, R.F., and Gillespie, J.W., "Relationship between Stoichiometry, Microstructure, and Properties of Amine-Cured Epoxies," *J. Appl. Polym. Sci.*, 71, 699 (1999).
- (29) Nguyen, T., Martin, J.W., Byrd, W.E., and Embree, N., "Relating Laboratory and Outdoor Exposures of Coatings: II. Effects of Relative Humidity on Photodegradation of Acrylic Melamine," *JOURNAL OF COATINGS TECHNOLOGY*, 74, No. 932, 31 (2002).
- (30) Burton, B.L., "Amine-Blushing Problems? No Sweat!," *Proc. Epoxy Resin Formulators' Meeting of The Society of the Plastics Industry*, July, 2001.
- (31) Pierce, P.E., and Schoff, C.K., "Coating Film Defects," *Federation Series on Coatings Technology*, Blue Bell, PA, pp. 7-24, 1998.
- (32) Sung, L., Karim, A., Douglas, J.F., and Han, C.C., "Dimensional Crossover in the Phase Separation Kinetics of Thin Polymer Blend Films," *Phys. Rev. Lett.*, 76, 4368-4371 (1996).
- (33) Koch, S.W., Desai, R.C., and Abraham, F.F., "Dynamics of Phase-Separation In Two-Dimensional Fluids—Spinodal Decomposition," *Phys. Rev. A: At., Mol., Opt. Phys.*, 27, 2152-2167 (1983).
- (34) Gu, X., Raghavan, D., Ho., D.L., Sung, L., VanLandingham, M.R., and Nguyen, T., "Nanocharacterization of Surface and Interface of Different Epoxy Networks," *Materials Research Society Symposium*, 710, DD10.9, 2002.
- (35) Gu, X., Martin, D., Martin, W.J., and Nguyen, T., "Surface, Interface, and Bulk Microstructure of Amine-Cured Epoxies—An Intensive AFM Study," *Proc. Adhesion Society Meeting*, M. Chaudhury (Ed.), p. 507, 2004.
- (36) Nguyen, T., Martin, J.W., Byrd, W.E., and Embree, N., "Relating Laboratory and Outdoor Exposures of Coatings: IV. Mode and Mechanism of Hydrolysis of Acrylic-Melamine Coatings," *JOURNAL OF COATINGS TECHNOLOGY*, 75, No. 941, 37 (2003).
- (37) Gu, X., Nguyen, T., Nguyen, D., and VanLandingham, M.R., "Surface and Interface Properties of PVDF/Acrylic Copolymer Blends," *Proc. Adhesion Society Meeting*, Orlando, FL, February, 2002.
- (38) Zhang, G., Pitt, W.G., Goates, S.R., and Owen, N.L., "Studies on Oxidative Photodegradation of Epoxy Resins by IR-ATR Spectroscopy," *J. Appl. Polym. Sci.*, 54, 419-427 (1994).